

Groundwater monitoring at a building site of the tidal flood protection system "MOSE" in the Lagoon of Venice, Italy

Original

Groundwater monitoring at a building site of the tidal flood protection system "MOSE" in the Lagoon of Venice, Italy / Casasso, A., DI MOLFETTA, A., Sethi, R.. - In: ENVIRONMENTAL EARTH SCIENCES. - ISSN 1866-6280. - ELETTRONICO. - (2015), pp. 2397-2408. [10.1007/s12665-014-3588-8]

Availability:

This version is available at: 11583/2560962 since:

Publisher:

Springer

Published

DOI:10.1007/s12665-014-3588-8

Terms of use:

This article is made available under terms and conditions as specified in the corresponding bibliographic description in the repository

Publisher copyright

(Article begins on next page)

26

27

28 groundwater monitoring

29 MOSE

30 dewatering

31 groundwater control

32 coastal aquifer

33 Venice

Keywords

34 **1 Introduction**

35 The city of Venice is known worldwide for its canals, its monuments and its unique cultural
36 heritage, but this fragile treasure is threatened by floods caused by high tides in the Adriatic Sea.
37 The best known part of the historical centre, Piazza San Marco, is also the most exposed, being
38 flooded about 50 times a year (Harleman, 2002). Besides the degradation of its artistic patrimony,
39 flooding in the historical centre of Venice impairs the quality of life of its inhabitants, contributing
40 to a massive migration towards the mainland.

41 In the last century, the severity and the frequency of flooding has been worsened by both eustatism
42 and man-induced subsidence, causing a relative sea level rise of 23 cm between 1908 and 1980
43 (Bras et al., 2001; Gatto and Carbognin, 1981). The sea level rising trend observed since the end of
44 19th century (1.8 ± 0.5 mm/year) is due to the Earth global warming (Bindoff et al., 2007).
45 Subsidence in the Venetian Lagoon, which has been monitored in the last 50 years by topographic
46 surveys (Carbognin et al., 1977) and, recently, by DGPS and SAR interferometry (Teatini et al.,
47 2005; Tosi et al., 2012; Tosi et al., 2009; Tosi et al., 2007), is also caused by the natural compaction
48 of the sediments and deep movements in the pre-Quaternary basement (Fontes and Bortolami,
49 1973), but the aquifer depressurization induced by water pumping in the Marghera industrial district
50 was the most important driving force until the Seventies (Carbognin et al., 1995). In the last 40
51 years, the groundwater extraction for industrial purposes has been drastically reduced with a
52 consequent stabilization of land subsidence in Venice and in the central lagoon. The northern and
53 southern parts, instead, are still being affected by this phenomenon due to pumping for agricultural
54 purposes, peat oxidation caused by reclamation work and geochemical compaction due to saltwater
55 intrusion (Tosi et al., 2009).

56 The most severe tidal flooding in Venice (+1.94 m at the tide gauge station of Punta della Salute)
57 occurred on November 4th 1966, inundating almost the whole historical centre (Di Molfetta and
58 Sethi, 2012). After this calamity, the Italian Government declared the safeguarding of Venice and

59 its lagoon as a national priority. The evaluation of technical alternatives took several years, and the
60 preliminary project phase started in the Eighties with the so-called Experimental Electro-mechanic
61 Module - MOSE (Fice and Scotti, 1990). The definitive project was approved in 2002, the
62 construction works started on September 2003 and their end is foreseen in 2016. The Venice
63 hydraulic safeguarding system is composed of four batteries of mobile barriers at the Lagoon's
64 inlets (Lido, Malamocco, Chioggia, see Fig. 1), which have to be lifted before the occurrence of
65 exceptional high tides (more than +1.10 m above mean sea level), isolating the Venetian Lagoon
66 from the sea (Cecconi, 1997). Rinaldo et al. (2008) proved the adequacy of the barriers for the
67 protection of Venice from floods, even during prolonged barrier closures, when a large runoff
68 volume is expected to be discharged into the Lagoon from its catchments. The raising of many
69 embankments and some modifications of the seawalls and coastal defences are also foreseen to
70 mitigate the effects of moderate storm surges (MOSE Venezia, 2013). Three harbours connected by
71 a lock gate are under construction at the Lagoon inlets, to ensure a navigation path while the
72 barriers are lifted (Fig. 2). Two of them, in Punta Sabbioni (Lido) and Ca' Roman (Chioggia), were
73 also used as provisional building sites for the concrete lodging caissons of mobile barriers, limiting
74 the soil occupation and the impact of the construction work on the mainland. The navigation lock of
75 Punta Sabbioni was used for this purpose for 5 years (January 2007 – March 2012), while the one in
76 Ca' Roman was dewatered from April 2008 to March 2014. Each of these basins was bounded by
77 slurry walls and cofferdams and drained by a system of dewatering wells. A possible adverse side
78 effect of groundwater control is represented by the depletion and depressurization of aquifers
79 outside the bounded area, that can also causes differential settlements (Powers et al., 2007) and
80 saltwater intrusion (Bear, 1999). For these reasons, groundwater monitoring activities were
81 therefore started in 2005 by Politecnico di Torino, under the supervision of CORILA¹, in order to

¹ Consortium for coordination of research activities concerning the Venice lagoon system.

82 assess the impact of the dewatering operations on the nearby area and aquifer system. The aim of
83 this study is to describe the groundwater monitoring program at the site of Punta Sabbioni, which
84 was completed on May 2013, with a focus on the criteria followed in the design of the monitoring
85 well network, on the choice of the measurements to be carried out and on the reaction of the aquifer
86 system to the natural and anthropogenic driving forces, as observed in almost 8 years of work.

87

88 **2 The monitored site**

89 The Punta Sabbioni construction site is located in the northern part of the Lagoon, at the Lido inlet,
90 on the edge of the Peninsula of Cavallino (Fig. 1 and Fig. 2). This land strip acquired its actual
91 shape after the construction of the seawalls of the Lido inlet (1907), which fostered the deposition
92 of sand transported by sea currents, and the land reclamation works with sand fillings (1930) which
93 transformed this marshland into a cropland. The harbour of Punta Sabbioni at the southern edge of
94 the Peninsula of Cavallino is composed of two basins connected by a navigation lock to allow the
95 boats to pass through the inlets when the mobile barriers are lifted. The southern basin (*tura*²) was
96 bounded by cofferdams (Fig. 2) and dried up starting from January 2007 by means of 18 dewatering
97 wells, 10 of them installed in the upper part of the boundary of the basin and 8 at the bottom. In this
98 way, a provisional construction site was created for the mobile gates, in which the groundwater
99 levels were kept below the elevation of the bottom (8.70m below mean sea level), to reduce the soil
100 occupancy on the mainland and the impact on the local main economical activities (greenhouse
101 horticulture and tourism). One of the main concerns about this technical solution was the impact on
102 the aquifers on the mainland, since a continuous dewatering pumping is required in order to keep
103 the groundwater level inside the basin below a safety threshold. A slurry wall was therefore dredged

² *Tura* is the ancient Venetian word to designate the bounded basins used for the wooden pole foundations of the palaces of Venice.

104 with the Cutter Soil Mixing technique to a depth of 28m, crossing both the shallow aquifers
105 (Bringiotti et al., 2008; Gerressen et al., 2008), with the aim of limiting the extension of the
106 drawdown cone, and a continuous groundwater level monitoring program was set up. The
107 dewatering operations lasted for 5 years and they were stopped on March 2012 to allow the
108 recovery of pristine conditions. After the drying up phase (January 2007), the dewatering discharge
109 was set to around 600 m³/d in order to keep the hydraulic head at 11 m below m.s.l. inside the
110 basin. In the following years, the safety threshold was elevated to 10 m below m.s.l., thus reducing
111 the total well flow rate to 550 m³/d in October 2009 and to 450 m³/d in September 2011, up to the
112 end of this activity in March 2012.

113 The shallow stratigraphy of the building site is composed of a sequence of sub-horizontal poorly
114 consolidated sedimentary layers, with different origin and grain size. The most superficial stratum,
115 layer A, is a silty sand with a thickness of 15m, that began to form during the Holocene sea
116 transgression (7000 years ago) and, more recently, its thickness has been increased by the land
117 reclamation works. It contains a phreatic aquifer which is extended all over the Peninsula of
118 Cavallino (Rapaglia et al., 2010), with an average hydraulic conductivity $K = 1.8 \cdot 10^{-5} \text{ m/s}$
119 (varying in the range $K = 4.7 \cdot 10^{-6} \div 2.8 \cdot 10^{-5} \text{ m/s}$) that was estimated with mechanical slug tests
120 (Di Molfetta and Sethi, 2012). The underlying strata were formed during the late Pleistocene
121 alluvial deposition, which took place until 18000 years BP (Strozzi et al., 2009; Tosi et al., 2007): a
122 clayey silt aquiclude (layer B) at a depth ranging from 15 to 20m separates the phreatic aquifer from
123 the confined one (layer C) at 20÷25m from ground surface level, with an average $K = 4.8 \cdot 10^{-6} \text{ m/s}$
124 (range: $K = 2.2 \div 6.9 \cdot 10^{-6} \text{ m/s}$). The 3D stratigraphy in Fig. 3 reproduces the spatial variation of
125 the thickness of the three shallow layers, and confirms that the aquiclude (layer B) does not show
126 spatial discontinuities which could connect the unconfined (layer A) and the confined aquifer (layer
127 C). Both these aquifers are local systems bounded by the Peninsula of Cavallino, while the
128 shallowest regional aquifer, according to the classification of Da Lio et al. (2013), ranges between

129 55 and 74 m below mean sea level and it is separated from layer C by a thick stratum of silt. Since it
130 is characterized by a low permeability and a high salinity, it is poorly exploited, unlikely the
131 underlying six aquifers (ranging from 81 to 340 m below m.s.l.) which are the main source of
132 drinking water, for agriculture and industry in the lagoon and in a large part of the Veneto Region.
133

134 **3 The monitoring activities**

135 A network of 11 monitoring stations, each one composed of two piezometers drilled into the aquifer
136 layers A (PS01÷PS11) and C (PP01÷PP11), was installed close to the building site on July 2005 (Di
137 Molfetta et al., 2005). The underlying aquifers have not been monitored, since they are separated by
138 a thick impervious layer and hence they are deemed to be not influenced by the construction work.
139 The observation wells (Fig. 2) were installed at a distance of 125m to 1100m from the centre of the
140 *tura* and of 15÷500m from the coastline, covering an area of about 70 hectares with a very high
141 spatial resolution. Three additional deep piezometers (PP12÷PP14) were installed in November
142 2008 to enhance the effectiveness of measurement of the spatial distribution of the hydraulic heads
143 close to the dewatered basin.

144 Coastal aquifers are usually very sensitive to climate driving forces, due to their low depth to water
145 table and to the influence of tides: consequently, a synchronous measurement of hydraulic heads is
146 vital for a correct representation of the flow field. Each well is therefore equipped with an automatic
147 pressure transducer acquiring data at a frequency of one measure every 10 minutes. Since
148 groundwater density is variable in the monitored aquifers, the water pressure (p) measured by
149 submerged data loggers is converted into freshwater hydraulic head, according to the following
150 formula (Post et al., 2007):

$$151 \quad h = z_i + \frac{p}{\rho_f g}$$

152 [1]

153 where $\rho_f = 1000 \text{ kg/m}^3$ is the freshwater density and $z_i = -6.036 \text{ m a.s.l.}$ is the reference
154 elevation, at which the transducers are installed.

155 The monitored aquifers are not exploited for human consumption or agriculture but, especially in
156 the phreatic aquifer, an increase in groundwater salinity induced by dewatering would be
157 detrimental for vegetation and crops. Chloride content and salinity are strongly correlated with the
158 electrical conductivity (EC) of groundwater (Cimino et al., 2008; El Moujabber et al., 2006;
159 Katznelson, 2004), and EC values are often used as a threshold for the acceptability of water for
160 irrigation purpose: for example, according to Lee and Song (2007), the limit is 2 mS/cm for most
161 species, and 15 mS/cm for the most salt-resistant ones. Monthly EC vertical profiles were therefore
162 measured using a multi-parametric probe, in order to study the evolution of the interface between
163 freshwater and salt water (saltwater wedge) and to ascertain if the dewatering activity in the *tura*
164 was triggering the saltwater intrusion on the mainland. Although water samplings give better detail
165 on groundwater geochemistry and how it varies through time, vertical EC profiles are much cheaper
166 and less time-consuming. In addition, they allow the vertical heterogeneity of groundwater salinity
167 to be assessed, e.g. in order to monitor the freshwater lens on which most plants rely for their
168 survival.

169 In order to assess the anthropogenic impacts on subsurface water, the data collected during almost
170 eight years of monitoring activity were compared with the natural driving forces (tidal oscillations,
171 rainfall and evapotranspiration). The time series of sea-water levels are acquired from the “Diga
172 Sud Lido” tidal gauge of ICPSM ³, at a frequency of one measure per hour. The mean sea level
173 amplitude in the Venice lagoon is 104 cm during spring tides and 46 cm during neap tides (Cucco
174 and Umgiesser, 2006), and their periods are respectively 6 and 12 hours. Due to its small depth to

³ ICPSM (Istituto Centro di Previsione e Segnalazione Maree) is the agency for the measurement and forecast of tides in the Venice Lagoon.

175 water table, ranging from some 0.30 m to 2.50 m, the dynamics of groundwater levels in the
176 phreatic aquifer are strongly affected by the infiltration and the evapotranspiration. Rainfall data are
177 registered on a hourly basis by the meteorological station “Cavallino Treporti” of ARPA Veneto ⁴,
178 at a distance of 5.5 km from the site. The climate of the Venetian lagoon is characterized by an
179 average annual precipitation of some 800 mm, and monthly rainfall height is almost uniform during
180 the year (Table 1), but storms are much more frequent during winter and spring, while few intense
181 thunderstorms occur in May and September.

182

183 **4 Monitoring results**

184 The data acquisition at the Punta Sabbioni building site started on October 11th, 2005 and ended on
185 April 30th, 2013. The *ante operam* situation was analyzed during the preliminary works, in order to
186 collect reference data which are essential for the assessment of groundwater control impacts
187 (Attanayake and Waterman, 2006). This phase lasted until March 2006, when a slurry wall and a
188 series of cofferdams were dredged, thus modifying the subsurface water circulation. The dewatering
189 of the *tura* lasted from January 2007 to March 2012 and, after the pumping cease, the *post operam*
190 monitoring program was carried on for the subsequent 14 months, up to the end of April 2013, in
191 order to verify the recovery to the pristine condition.

192 **4.1 Hydraulic heads**

193 The *ante operam* monitoring phase allowed two different types of groundwater level dynamics in
194 the phreatic aquifer to be distinguished, depending on the distance of the piezometers from the
195 coastline (Casasso et al., 2009). Along a narrow belt of less than 100 meters from the coastline, sea
196 tides are the strongest driving force acting on the phreatic aquifer. Forced oscillations are observed

⁴ ARPA Veneto is the regional environmental protection agency.

197 in PS01, PS02 (Fig. 4) and, in the *ante operam* phase (October 2005 - March 2006), also in PS03
198 and PS04 (Fig. 5), with a slight delay of 1-2 hours between the peaks of the sea and groundwater
199 levels. The Tidal Efficiency Factor (TEF), which is the ratio between the standard deviation of the
200 hydraulic heads in the piezometer and of the sea levels (Erskine, 1991), were calculated for the
201 coastal piezometers in the phreatic aquifer (PS01÷PS04) and in the confined one (PP01÷PP04),
202 differentiating between spring and neap tide periods (see Table 2). The values of this coefficient
203 range approximately between 40 and 50% in the phreatic aquifer, and between 15 and 30% in the
204 confined one. The TEF values of PS03, PS04 (and, to a lesser extent, PP03 and PP04) experienced a
205 strong reduction during the construction works, confirming that the tide-induced oscillations have
206 been dampened, as shown in Fig. 5, due to the emplacement of the slurry wall of the *tura* on March
207 2006. Groundwater levels in these piezometers now show the same behaviour observed in the
208 mainland (PS05÷PS11, see Fig. 2b), where sudden level increases occur after rainfall events and a
209 strong evapotranspiration is observed, especially in the Summer season, due to the small depth to
210 water table (i.e. 0.3 m to 2.5 m) of the phreatic aquifer (Fig. 6). The influence of sea level
211 fluctuations is negligible, since the amplitude of tide-induced oscillations exponentially decays with
212 the distance from the coastline (Erskine, 1991; Li et al., 2002).

213 The cross-correlation suggested by Song and Zemansky (2012, 2013) is a powerful tool to assess
214 and compare the influence of different driving forces on groundwater levels, and it was applied to
215 analyze the influence of rainfall and tides on the hydraulic heads during a wet month (March 2009,
216 with a total rainfall height of 122.4 mm) and a dry month (July 2009, with a cumulate precipitation
217 of 7 mm). Plots reported in the supporting information confirm that, in the phreatic aquifer, the
218 most important driving force is rainfall, except for the coastal piezometers PS01 and PS02, where
219 tidal oscillations are prevailing. On the other hand, in the confined aquifer, rainfall events exert an
220 appraisable impact only for a mainland monitoring well (PP07), probably due to the formation of
221 ponds, while tides are an important driving force for levels in PP01 and PP02. Close to the *tura*

222 (PP03, PP04, PP12, PP13, PP14), hydraulic heads are almost insensitive to tides and precipitations,
223 since the impact of dewatering pumping was dominating.

224 Forward Neural Networks (FNNs) carried out by Taormina et al. (2012) confirmed the deductions
225 about the driving forces acting on the shallow aquifer, since a good fit was achieved when
226 forecasting the hydraulic heads in the mainland piezometer PS10 only with climate data (rainfall
227 and estimated evapotranspiration).

228 The shallow aquifer is characterized by a small depth to water table, and the cross-correlation plots
229 reported in the supporting information confirm that a reduced time lag (i.e. smaller than 24 h) is
230 observed between a rainfall event and a groundwater level peak. The level rises (Δh) against every
231 appraisable rainfall event (cumulate height $h > 5mm$) were calculated for all the monitoring year
232 2009, and their ratios (Table 3) give a good indication of the local effective porosity of the aquifer,
233 which is deemed to be quite heterogeneous due to the recent formation of the phreatic aquifer layer.
234 In the monitored period, a strong depletion of the phreatic aquifer occurred during the Summer
235 droughts of 2007, 2009 and 2012. Further surveys demonstrated a strong correlation between
236 groundwater levels and rainfall on a monthly and yearly basis (Fig. 7), but no direct effect of
237 pumping was observed in the shallow aquifer, since the hydraulic heads in the phreatic aquifer and
238 in the confined one in the most impacted monitoring position (PS04-PP04) do not show any
239 correlation (Fig. 8).

240 **4.2 Electrical Conductivity (EC) vertical profiles**

241 The strong evapotranspiration occurring during Summer season also influences the seasonal
242 evolution of the EC profiles, as shown in Fig. 9, due to the lowering of the water table and, to a
243 lesser extent, to the reduced volume of groundwater in which the salts are dissolved. Indeed, the
244 position of the saltwater wedge depends on the water table elevation and, according to the Badon-
245 Ghyben-Herzberg formula (Bear, 1999):

246
$$\xi = \frac{\rho_f}{(\rho_s - \rho_f)} h_f \approx 30 \div 40 h_f$$

247 [2]

248 where ρ_f and ρ_s are respectively the density of freshwater and saltwater, h_f is the water table
249 elevation and ξ is the depth of the interface between the freshwater and the underlying saltwater.

250 Using typical values of freshwater (1000 kg/m^3) and saltwater ($1025 \div 1033 \text{ kg/m}^3$) density, one
251 can easily understand that a small reduction of groundwater level results in a noticeable
252 displacement of the saltwater wedge (i.e. 30 to 40 times larger).

253 In the inner area (PS05, PS06, PS07, PS09, PS10, PS11), where groundwater levels are usually
254 higher than on the coastline, the conductivity is almost uniform along the well column, with low
255 values ($0.3 - 2 \text{ mS/cm}$) typical of fresh or slightly brackish water. Also coastal piezometers (PS01,
256 PS02) have a uniform profile, but larger EC values are observed ($10 \div 15 \text{ mS/cm}$). In PS03, PS04
257 and PS08, the profiles show an abrupt EC variation from freshwater ($1 \div 2 \text{ mS/cm}$) to saltwater
258 ($8 \div 25 \text{ mS/cm}$), which also occurs in PS09 and PS10 during summer due to the saltwater intrusion.

259 The shape of the EC profile can vary during the year, generally with a temporary saltwater intrusion
260 occurring in Summer and Autumn (Fig. 9) which sometimes involves the whole aquifer depth, e.g.
261 in the piezometers PS05 and PS10. No permanent salinization trends were observed, while a clear
262 desalinization trend was assessed for PS03 and PS04 (Fig. 10), due to the dam effect generated by
263 the impermeable slurry wall of the *tura*, except for 2012 due to a severe Summer drought (see Fig.
264 7) and a consequent strong water table level decrease.

265 The EC profiles are in good agreement with those of Rapaglia et al. (2010), who observed values
266 between 1 and 14 mS/cm in two sites in the Peninsula of Cavallino, one in Punta Sabbioni (some
267 800 m northward from PS09-PP09) and one in Treporti (some 3 km from the monitored site). In
268 particular, they found a shallow freshwater lens in Punta Sabbioni but not in Treporti, inferring that

269 this is due to a smaller Submarine Groundwater Discharge (and hence, a smaller saltwater supply
270 from the sea side of the Peninsula) in this site.

271

272 **4.3 Groundwater control in the tura**

273 The EC monitoring in the shallow aquifer confirmed that no significant influence was exerted by
274 the dewatering pumping in the tura, as one can also observe comparing the hydraulic heads in the
275 piezometers PS04 (shallow) and PP04 (deep) in Fig. 8. On the other hand, the effects of this activity
276 on the deep aquifer level are evident: the drawdown induced by dewatering pumping in the building
277 site reached its maximum in piezometers PP04 (4 to 6 m) and PP03 (2.5 to 3.5 m), located behind
278 the slurry wall, with a logarithmic decay with the increasing distance from the centre of the tura
279 (Fig. 11). The radius of the depression cone induced by dewatering operations reached an extent of
280 about 1 km around the building site, which is not uncommon for dewatered basins of such a large
281 dimension (Wang et al., 2013). The absence of any evident drawdown in the shallow aquifer is due
282 to the presence of a confining clayey aquiclude (layer B) with no evident spatial discontinuities
283 (Fig. 3), that prevents any vertical connection with the underlying dewatered confined aquifer, and
284 the slurry wall of the *tura* also proved to be successful in preventing such a heavy environmental
285 impact. The monitoring results were communicated monthly to CORILA and allowed the
286 optimization of the discharge distribution of the dewatering wells and a reduction of the impact on
287 the monitored mainland side. The oscillations of the hydraulic head were reduced through the years
288 and a slight level recovery was also achieved (Fig. 8) due to the aforementioned variation of the
289 safety threshold in the groundwater controlled basin, which was switched from 11 to 10m below
290 m.s.l. in October 2009. Nevertheless, the dewatering pumping caused some local settlements in the
291 immediate vicinity of the building site (6÷10 cm in PP03 and PP04, at less than 200 m from the
292 centre of the tura), which have been quantified by periodic plano-altimetric surveys on the
293 piezometers. These ground surface displacements are due to the compaction of the silty and clayey

294 component of the aquifer and of the overlying aquiclude caused by the increase of the effective
295 stresses induced by pumping operations. Minor displacements have been found in the other
296 monitoring wells. The extension of the major land settlements shows good agreement with the
297 TerraSAR-X images interferometric analyses conducted by Strozzi et al. (2009) and Tosi et al.
298 (2012).

299 The dewatering pumping in the building site of Punta Sabbioni was interrupted on March 3, 2012.
300 The southern basin of the navigation lock was flooded, and the hydraulic heads in the deep aquifer
301 definitely recovered to the *ante operam* spatial distribution in August 2012 (Fig. 11). In the phreatic
302 aquifer, no significant variations were observed during the post-pumping recovery phase,
303 confirming that it was not affected by the dewatering activity. The *post operam* monitoring phase
304 ended on April 30, 2013. The hydraulic head are still measured by the automatic acquisition
305 network, although no reports are being published now.

306

307 **5 Conclusions**

308 In this paper, the results of the groundwater monitoring in the *MOSE* building site of Punta
309 Sabbioni, in the Venetian Lagoon, are described. The impact of the construction work on the aquifer
310 system is related to the dewatering operations conducted inside a wide basin, formerly occupied by
311 the sea, that was used for the construction of the mobile gates and will later serve as a navigation
312 lock when the barriers are lifted. The hydraulic heads in the surrounding area were monitored by a
313 network of monitoring wells screened in the shallow and in a confined aquifer layer.

314 Although an impermeable slurry wall barrier was excavated to limit the impact on the aquifer
315 system and proved to be successful in avoiding an impact on the phreatic aquifer, the monitoring
316 network revealed a drawdown cone in the confined aquifer extending to 1 km from the southern
317 basin of the harbour during a period of five years (January 2007 - March 2012). After the

318 interruption of the dewatering pumping, the hydraulic heads in the deep aquifer returned to the *ante*
319 *operam* spatial distribution in five months.

320 During the eight years of the monitoring program, no adverse effects were observed in the phreatic
321 aquifer, which is mainly influenced by the tides on a narrow strip along the coastline and by the
322 climate - precipitation and evapotranspiration - on the mainland. Droughts were observed in the
323 Summer seasons of 2007, 2009 and 2012, but the comparison with climate data confirmed the
324 absence of a depletion induced by the construction works.

325 The slurry wall of the *tura* had a positive effect of desalinization in a portion of the phreatic aquifer,
326 which is isolated from seawater intrusion, as confirmed by monthly EC measurement campaigns.
327 Subsidence has been observed on a narrow strip along the *tura*, which has been confirmed by both
328 GPS surveys and SAR interferometry (Strozzi et al., 2009; Tosi et al., 2012).

329 The monitoring activity proved to be successful in evidencing the impacts of construction work by
330 ascertaining the effects of the natural driving forces influencing the hydrogeology of the area of the
331 building site. In particular, continuous hydraulic head recording permitted a clear and rigorous
332 representation of the groundwater flow field, especially in the phreatic aquifer, which is subject to
333 rapid variations in response to natural driving forces. The monthly vertical EC profiles permitted
334 the saltwater intrusion to be monitored with a simple, fast and inexpensive method with high spatial
335 resolution. Periodic reports and a strong feedback procedure with the contractors of the worksite
336 proved to be effective in reducing the groundwater impact induced by the construction of this
337 infrastructure.

338 **Acknowledgments**

339 The authors wish to thank Dr. Pierpaolo Campostrini and Dr. Caterina Dabalà of CORILA
340 (Consortium for coordination of research activities concerning the Venice lagoon system), the
341 Ministero delle Infrastrutture e dei Trasporti - Magistrato alle Acque di Venezia (Ministry of
342 Infrastructures and Transports - Venice Water Authority) for the permission to use the data of the
343 monitoring program B.6.72 B/1÷8 (Survey and monitoring activities of the effects of the
344 construction works at the Lagoon inlets).

345 The authors gratefully acknowledge Silvia Delforno, Chiara Santi and Tommaso Baldarelli, who
346 collaborated on this project at the early stages.

References

- 347
348
- 349 Attanayake PM, Waterman MK (2006) Identifying environmental impacts of underground
350 construction. *Hydrogeology Journal* 14:1160-1170. doi:DOI 10.1007/s10040-006-0037-0
- 351 Bear J (1999) *Seawater intrusion in coastal aquifers : concepts, methods, and practices*. Kluwer
352 Academic, Dordrecht ; Boston
- 353 Bindoff NL, Willebrand J, Artale V, Cazenave A, Gregory JM, Gulev S, Hanawa K, Le Quéré C,
354 Levitus S, Nojiri Y, Shum CK, Talley LD, Unnikrishnan AS (2007) Observations: Oceanic Climate
355 Change and Sea Level. In: IPCC (ed), *Climate Change 2007: The Physical Science Basis*
356 Contribution of Working Group I to the Fourth Assessment Report of the Intergovernmental Panel
357 on Climate Change Cambridge University Press, Cambridge (U.K.) and New York (USA). p 387
- 358 Bras RL, Harleman DRF, Rinaldo A, Rizzoli P (2001) Rescuing Venice from a watery grave.
359 *Science* 291:2315-2315.
- 360 Bringiotti M, Dossi M, Nicastro D (2008) Miscelazione profonda dei terreni. Metodi classici e
361 tecnologie innovative – CSM by Bauer. Geofluid, Piacenza (Italy)
- 362 Carbognin L, Gambolati G, Ricceri G (1977) New trend in the subsidence of Venice. IAHS
363 Symposium, Anaheim (USA). pp 65-81
- 364 Carbognin L, Marabini S, Tosi L (1995) Land subsidence and degradation of the Venice littoral
365 zone, Italy. In: IAHS (ed), *5th International Symposium on Land Subsidence*, Den Haag
366 (Netherlands). pp 391-402
- 367 Casasso A, Di Molfetta A, Sethi R (2009) Monitoring plan of MOSE building sites (Venezia): the
368 hydrogeologic situation around the building sites., *Riunione Annuale CORILA*, Venice (Italy). pp
369 217-226
- 370 Cecconi G (1997) The Venice lagoon mobile barriers. Sea level rise and impact of barrier closures.,
371 *Italian Days of Coastal Engineering*, Venice (Italy)
- 372 Cimino A, Cosentino C, Oieni A, Tranchina L (2008) A geophysical and geochemical approach for
373 seawater intrusion assessment in the Acquedolci coastal aquifer (Northern Sicily). *Environmental*
374 *Geology* 55:1473-1482. doi:10.1007/s00254-007-1097-8
- 375 Cucco A, Umgiesser G (2006) Modeling the Venice lagoon residence time. *Ecological Modelling*
376 193:34-51. doi:10.1016/j.ecolmodel.2005.07.043
- 377 Da Lio C, Tosi L, Zambon G, Vianello A, Baldin G, Lorenzetti G, Manfè G, Teatini P (2013) Long-
378 term groundwater dynamics in the coastal confined aquifers of Venice (Italy). *Estuarine, Coastal*
379 *and Shelf Science* 135:248-259. doi:<http://dx.doi.org/10.1016/j.ecss.2013.10.021>
- 380 Di Molfetta A, Sethi R (2012) *Ingegneria degli acquiferi*. Springer
- 381 Di Molfetta A, Sethi R, Delforno S, Lingua A, Tonolo FG, Piras M (2005) Rapporto di
382 Pianificazione Operativa. Area: Suolo. Macroattività: Livelli di falda., Studio B672 B/1 Attività di
383 rilevamento per il monitoraggio degli effetti prodotti dalla costruzione delle opere alle bocche

- 384 lagunari. Politecnico di Torino - DITAG and CORILA (Consortium for coordination of research
385 activities concerning the Venice lagoon system). p 103
- 386 El Moujabber M, Samra BB, Darwish T, Atallah T (2006) Comparison of Different Indicators for
387 Groundwater Contamination by Seawater Intrusion on the Lebanese Coast. *Water Resour Manage*
388 20:161-180. doi:10.1007/s11269-006-7376-4
- 389 Erskine AD (1991) The Effect of Tidal Fluctuation on a Coastal Aquifer in the UK. *Ground Water*
390 29:556-562. doi:10.1111/j.1745-6584.1991.tb00547.x
- 391 Fice JL, Scotti A (1990) The Flood-Prevention Scheme of Venice: Experimental Module. *Water*
392 *and Environment Journal* 4:70-77. doi:10.1111/j.1747-6593.1990.tb01559.x
- 393 Fontes JC, Bortolami G (1973) Subsidence of Venice Area during Past 40,000 Yr. *Nature* 244:339-
394 341.
- 395 Gatto P, Carbognin L (1981) The Lagoon of Venice: natural environmental trend and man-induced
396 modification. *Bulletin des Sciences Hydrologiques* 26:379-391.
- 397 Gerressen FW, Schoepf M, Stoetzer E, Fiorotto R (2008) Cutter Soil Mixing (CSM) on the MOSE
398 Project - Venice, Italy. *Tiefbau* 6:330-333.
- 399 Harleman DRF (2002) Saving Venice from the sea. The Pennsylvania State University - College of
400 Engineering, University Park, PA (USA)
- 401 Katznelson R (2004) Conductivity/Salinity Measurement Principles and Methods. The Clean Water
402 Team Guidance Compendium for Watershed Monitoring and Assessment. Clean Water Team,
403 Division of Water Quality, California State Water Resources Control Board (SWRCB),
404 Sacramento, CA. pp 1-9
- 405 Lee J-Y, Song S-H (2007) Evaluation of groundwater quality in coastal areas: implications for
406 sustainable agriculture. *Environmental Geology* 52:1231-1242. doi:10.1007/s00254-006-0560-2
- 407 Li HL, Jiao JJ, Luk M, Cheung KY (2002) Tide-induced groundwater level fluctuation in coastal
408 aquifers bounded by L-shaped coastlines. *Water Resources Research* 38:-.
409 doi:10.1029/2001wr000556
- 410 MOSE Venezia (2013) Activities for the safeguarding of Venice and its lagoon.
- 411 Post V, Kooi H, Simmons C (2007) Using hydraulic head measurements in variable-density ground
412 water flow analyses. *Ground Water* 45:664-671. doi:DOI 10.1111/j.1745-6584.2007.00339.x
- 413 Powers JP, Corwin AB, Schmall PC, Kaeck WE (2007) Construction dewatering and groundwater
414 control. New methods and applications. Third edition.
- 415 Rapaglia J, Di Sipio E, Bokuniewicz H, Zuppi GM, Zaggia L, Galgaro A, Beck A (2010)
416 Groundwater connections under a barrier beach: A case study in the Venice Lagoon. *Continental*
417 *Shelf Research* 30:119-126. doi:DOI 10.1016/j.csr.2009.10.001
- 418 Rinaldo A, Nicotina L, Celegon EA, Beraldin F, Botter G, Carniello L, Cecconi G, Defina A, Settin
419 T, Uccelli A, D'Alpaos L, Marani M (2008) Sea level rise, hydrologic runoff, and the flooding of
420 Venice. *Water Resources Research* 44:-. doi:10.1029/2008wr007195

- 421 Song S-H, Zemansky G (2012) Vulnerability of groundwater systems with sea level rise in coastal
422 aquifers, South Korea. *Environ Earth Sci* 65:1865-1876. doi:10.1007/s12665-011-1169-7
- 423 Song S-H, Zemansky G (2013) Groundwater level fluctuation in the Waimea Plains, New Zealand:
424 changes in a coastal aquifer within the last 30 years. *Environ Earth Sci* 70:2167-2178.
425 doi:10.1007/s12665-013-2359-2
- 426 Strozzi T, Teatini P, Tosi L (2009) TerraSAR-X reveals the impact of the mobile barrier works on
427 Venice coastland stability. *Remote Sensing of Environment* 113:2682-2688.
428 doi:10.1016/j.rse.2009.08.001
- 429 Taormina R, Chau K-w, Sethi R (2012) Artificial neural network simulation of hourly groundwater
430 levels in a coastal aquifer system of the Venice lagoon. *Engineering Applications of Artificial*
431 *Intelligence* 25:1670-1676. doi:<http://dx.doi.org/10.1016/j.engappai.2012.02.009>
- 432 Teatini P, Tosi L, Strozzi T, Carbognin L, Wegmuller U, Rizzetto F (2005) Mapping regional land
433 displacements in the Venice coastland by an integrated monitoring system. *Remote Sensing of*
434 *Environment* 98:403-413. doi:DOI 10.1016/j.rse.2005.08.002
- 435 Tosi L, Teatini P, Bincoletto L, Simonini P, Strozzi T (2012) Integrating Geotechnical and
436 Interferometric SAR Measurements for Secondary Compressibility Characterization of Coastal
437 Soils. *Surv Geophys* 33:907-926. doi:DOI 10.1007/s10712-012-9186-y
- 438 Tosi L, Teatini P, Carbognin L, Brancolini G (2009) Using high resolution data to reveal depth-
439 dependent mechanisms that drive land subsidence: The Venice coast, Italy. *Tectonophysics*
440 474:271-284. doi:10.1016/j.tecto.2009.02.026
- 441 Tosi L, Teatini P, Carbognin L, Frankenfield J (2007) A new project to monitor land subsidence in
442 the northern Venice coastland (Italy). *Environmental Geology* 52:889-898. doi:10.1007/s00254-
443 006-0530-8
- 444 Wang J, Feng B, Yu H, Guo T, Yang G, Tang J (2013) Numerical study of dewatering in a large
445 deep foundation pit. *Environ Earth Sci* 69:863-872. doi:10.1007/s12665-012-1972-9
- 446

447

Tables

448

449 Table 1 - Average climatic parameters in Venice meteorological station "ARPAV-Cavallino

450 Treporti" , years 1992-2012).

Month	Total rainfall (mm)	Rainy days (h>1mm)
January	43.2	5/31
February	45.8	4/28
March	48.9	5/31
April	71.7	8/30
May	72.6	7/31
June	65.2	6/30
July	54.3	5/31
August	72.6	6/31
September	101.6	6/30
October	97.7	6/31
November	90.3	8/30
December	72.6	8/31
TOTAL	836.5 mm	74/365

451

452

453 Table 2 - Calculation of Tidal Efficiency Factors (TEF) during spring and neap tides, before (*ante*
 454 *operam*) and during the construction works.

Piezometer	Phase	x (m)	Tidal Efficiency Factors (-)	
			spring	neap
PS01	Ante operam	14	0.322	0.384
	During works	14	0.392	0.502
PS02	Ante operam	21	n.a.	n.a.
	During works	21	0.421	0.527
PS03	Ante operam	21	0.345	0.501
	During works	21	0.050	0.092
PS04	Ante operam	14	0.149	0.351
	During works	14	0.047	0.088
PP01	Ante operam	14	0.162	0.225
	During works	14	0.161	0.197
PP02	Ante operam	21	0.136	0.208
	During works	21	0.099	0.140
PP03	Ante operam	21	0.101	0.199
	During works	21	0.080	0.122
PP04	Ante operam	14	0.231	0.298
	During works	14	0.129	0.186

455

456

457 Table 3 - Comparison of mean ratios between rainfall height (h) and level rises in internal
 458 piezometers (ΔH) after rainfall events, and coefficients of relation (R^2).

Piezometer	PS03	PS04	PS05	PS06	PS07	PS09	PS10	PS11
$h / \Delta h$	0.096	0.143	0.126	0.080	0.090	0.163	0.162	0.129
R^2	0.856	0.875	0.863	0.826	0.800	0.729	0.880	0.855

459

Figure captions

460
461
462 Fig. 1 - Map of the Venetian Lagoon showing the main rivers, the urban centres and the MOSE
463 construction sites at the Lido, Malamocco and Chioggia inlets.
464
465 Fig. 2 - The building site (a) of Punta Sabbioni, located in the north-eastern part of the Lido's inlet,
466 and the detail of the dewatered basin and the groundwater monitoring network (b) of the site, which
467 is composed of 14 monitoring stations (black circles): all of them are equipped with a piezometer
468 screened in the deep aquifer (PP01÷PP14) and 11 of them with a shallow piezometer (PS01÷PS11).
469 The groundwater control system is composed of 18 wells, 10 of them installed in the upper part of
470 the boundary of the basin (red squares) and 8 wells at the bottom (blue triangles).
471
472 Fig. 3 – Cross-sections of the shallow stratigraphy of Punta Sabbioni (0÷29 m from the ground
473 surface), deduced by core samplings acquired during the drilling of the deep piezometers
474 (PP01÷PP11) and by the Province of Venezia (1656, 1697, LSM6, LST1). Three layers are
475 represented: the phreatic aquifer (layer A, cyan), the aquiclude (layer B, brown) and the shallow
476 confined aquifer (layer C, grey).
477
478 Fig. 4 - Response of a coastal piezometer (PS02) to tidal oscillations.
479
480 Fig. 5 - Evolution of the hydraulic heads pattern in the coastal piezometer PS03: since March 2006,
481 the emplacement of the slurry wall of the *tura* caused an abrupt interruption of tide-induced
482 oscillations.
483

484 Fig. 6 - Time series of the hydraulic heads in the shallow piezometer PS10, during January 2009:
485 the level rise after rainfall events is almost immediate, due to the small depth to water table (< 2 m).

486

487 Fig. 7 - Comparison between the monthly cumulate rainfall height and the monthly average
488 hydraulic heads in the phreatic aquifer during the monitoring period (October 2005 - April 2013).

489

490 Fig. 8 - Comparison between hydraulic heads in the deep piezometer PP04 and in its homologue in
491 the shallow aquifer (PS04): no relation was observed comparing their dynamics, confirming the
492 absence of any depletion of the shallow aquifer due to the construction works.

493

494 Fig. 9 - Seasonal evolution of groundwater specific electrical conductivity (EC) vertical profiles in
495 PS06 (June 2012 - May 2013). Saltwater intrusion occurs in Summer and Autumn, while rainfall
496 infiltration from Autumn to Spring results in a noticeable decrease of EC.

497

498 Fig. 10 - Temporal evolution of groundwater specific electrical conductivity (EC) vertical profiles
499 in PS04. The significant decrease in conductivity, and hence salinity, is due to the isolation effect of
500 the slurry wall of the *tura*. An exception is observed in 2012, as the severe Summer drought caused
501 a strong saltwater intrusion, which was also observed in the other shallow piezometers.

502

503 Fig. 11 - Comparison between piezometric surfaces in the confined aquifer before the beginning of
504 dewatering pumping (October 2005, *ante operam* phase), during the groundwater control activity in
505 the *tura* (November 2010) and after it was ceased (April 2013, *post operam* phase).

Figure 1
[Click here to download high resolution image](#)

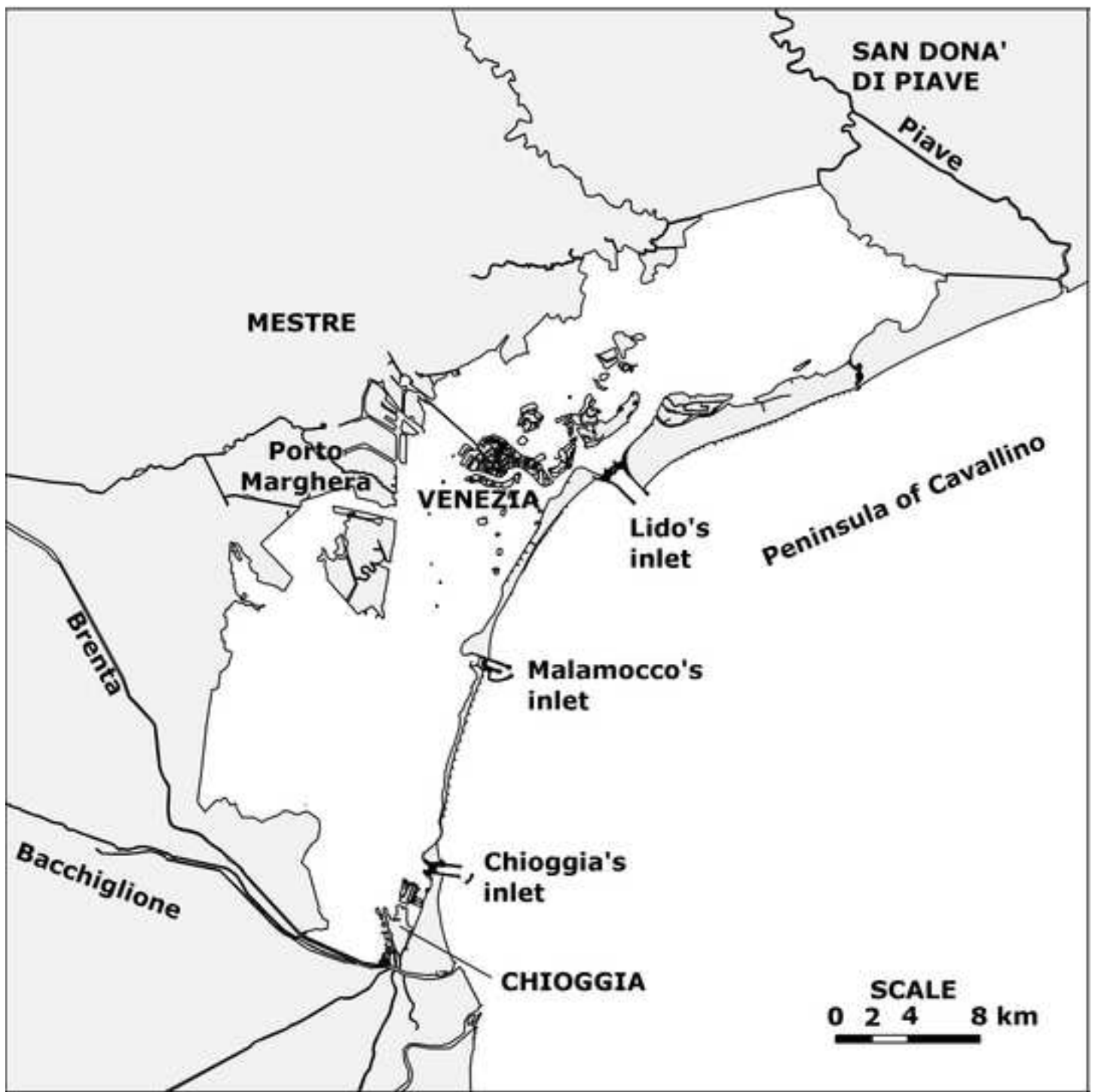


Figure 2
[Click here to download high resolution image](#)

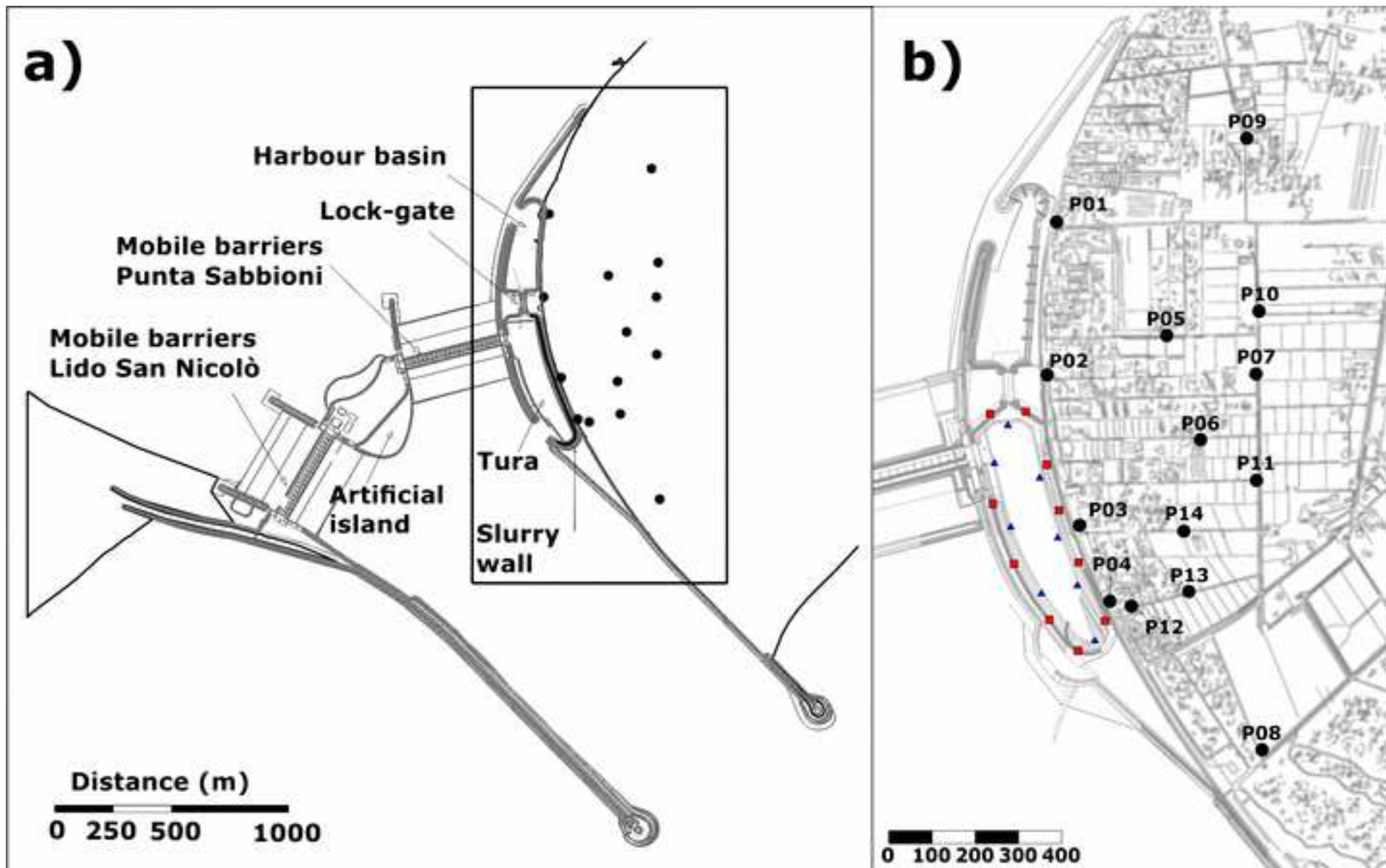


Figure 3
[Click here to download high resolution image](#)

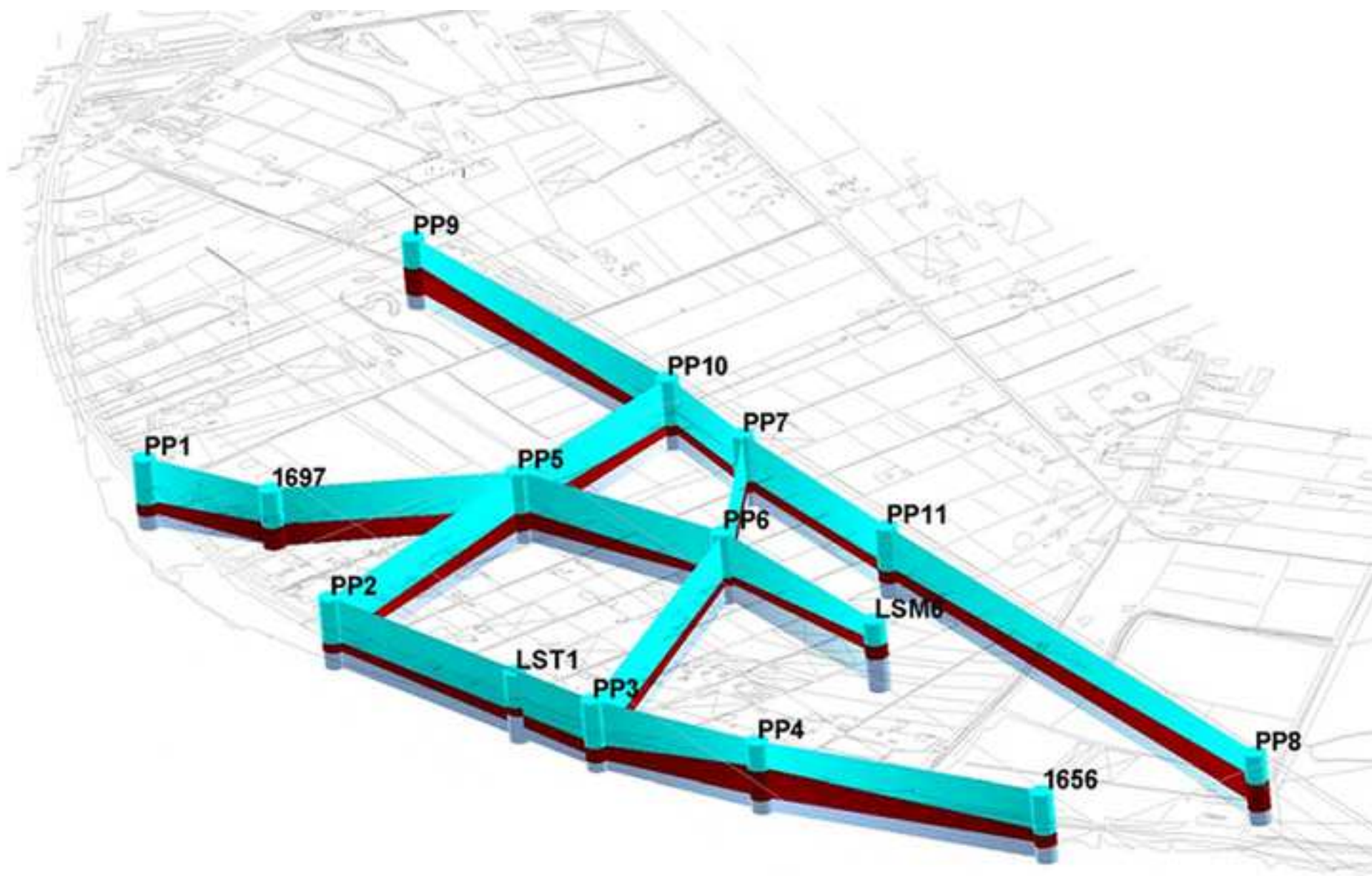


Figure 4

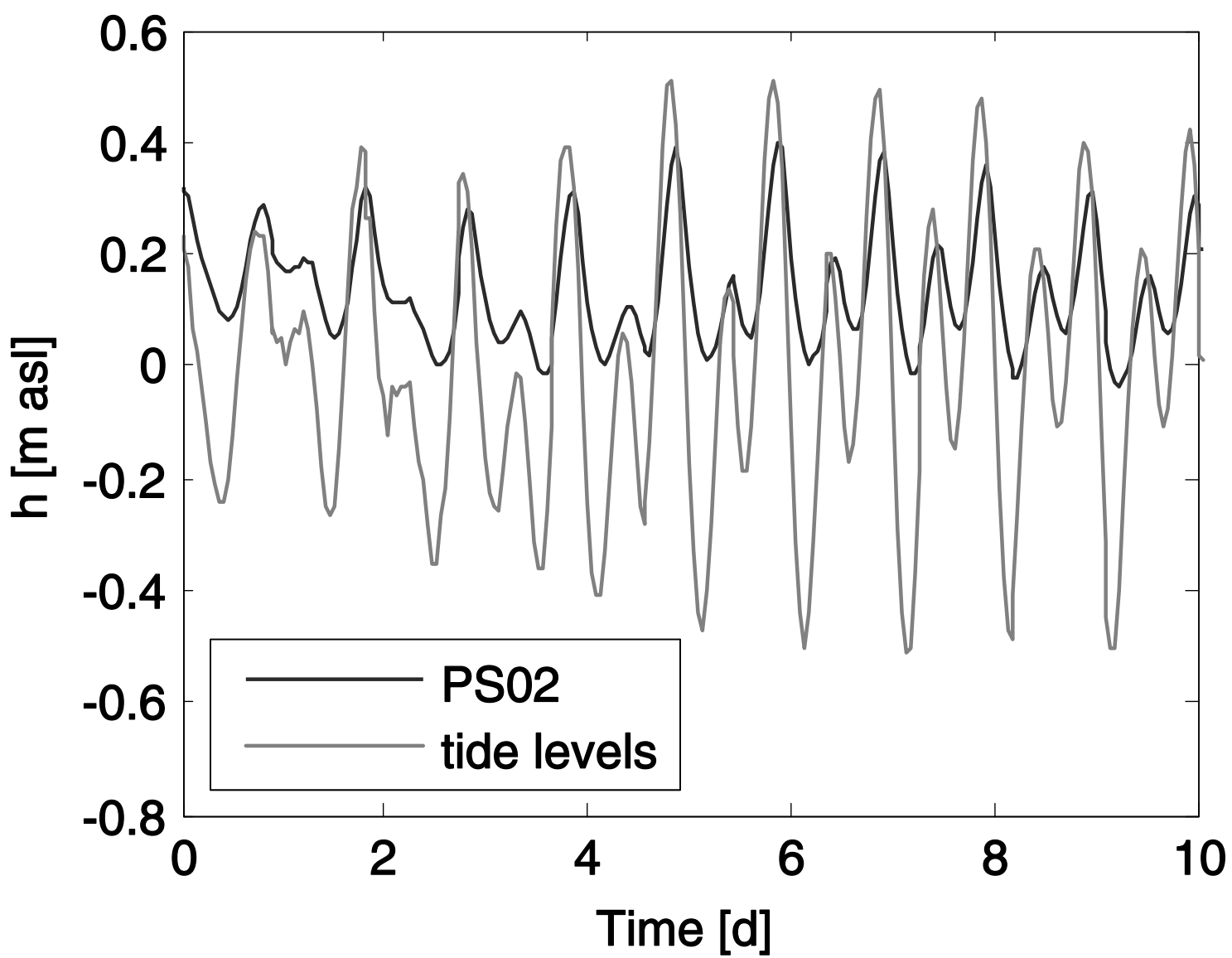


Figure 5

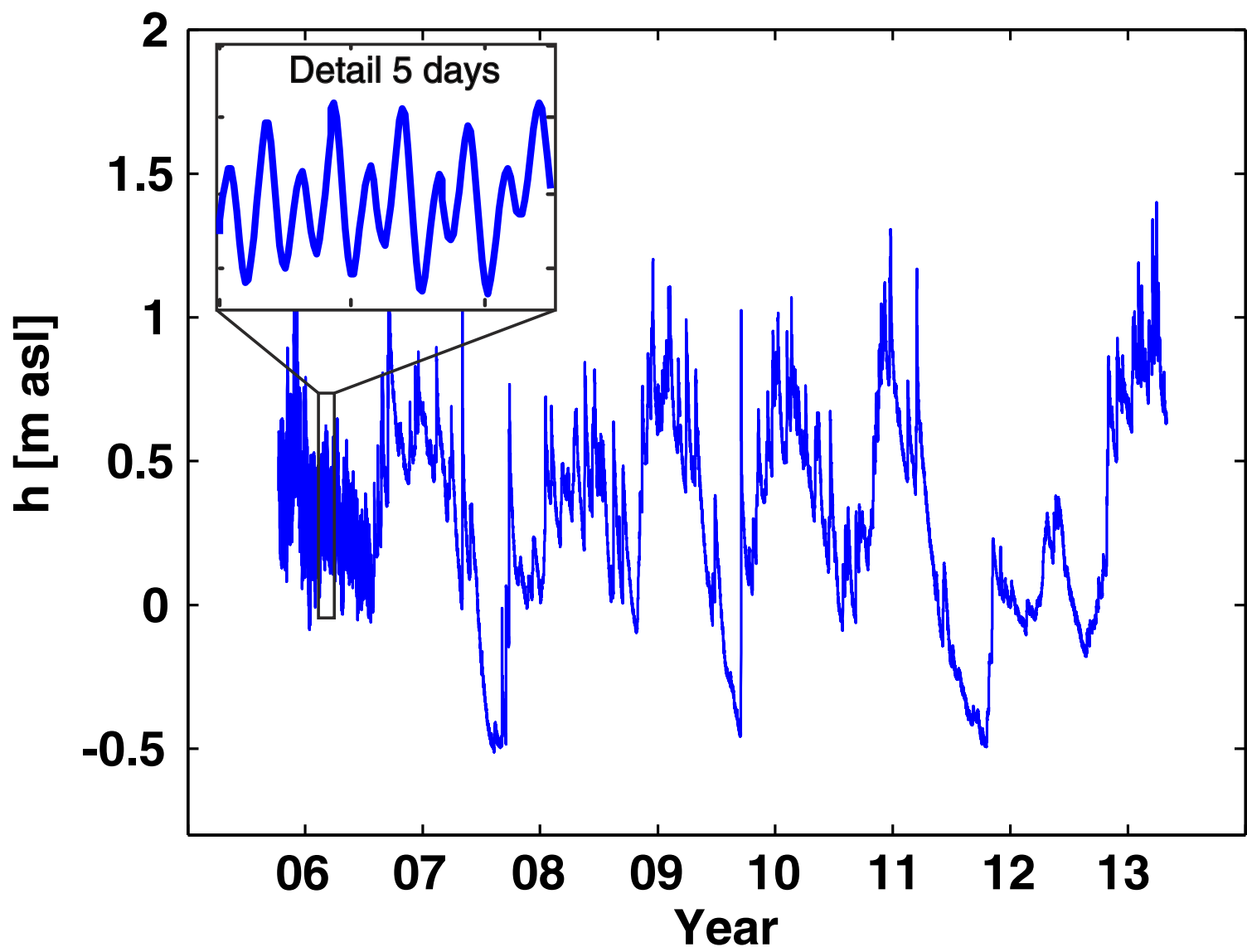


Figure 6

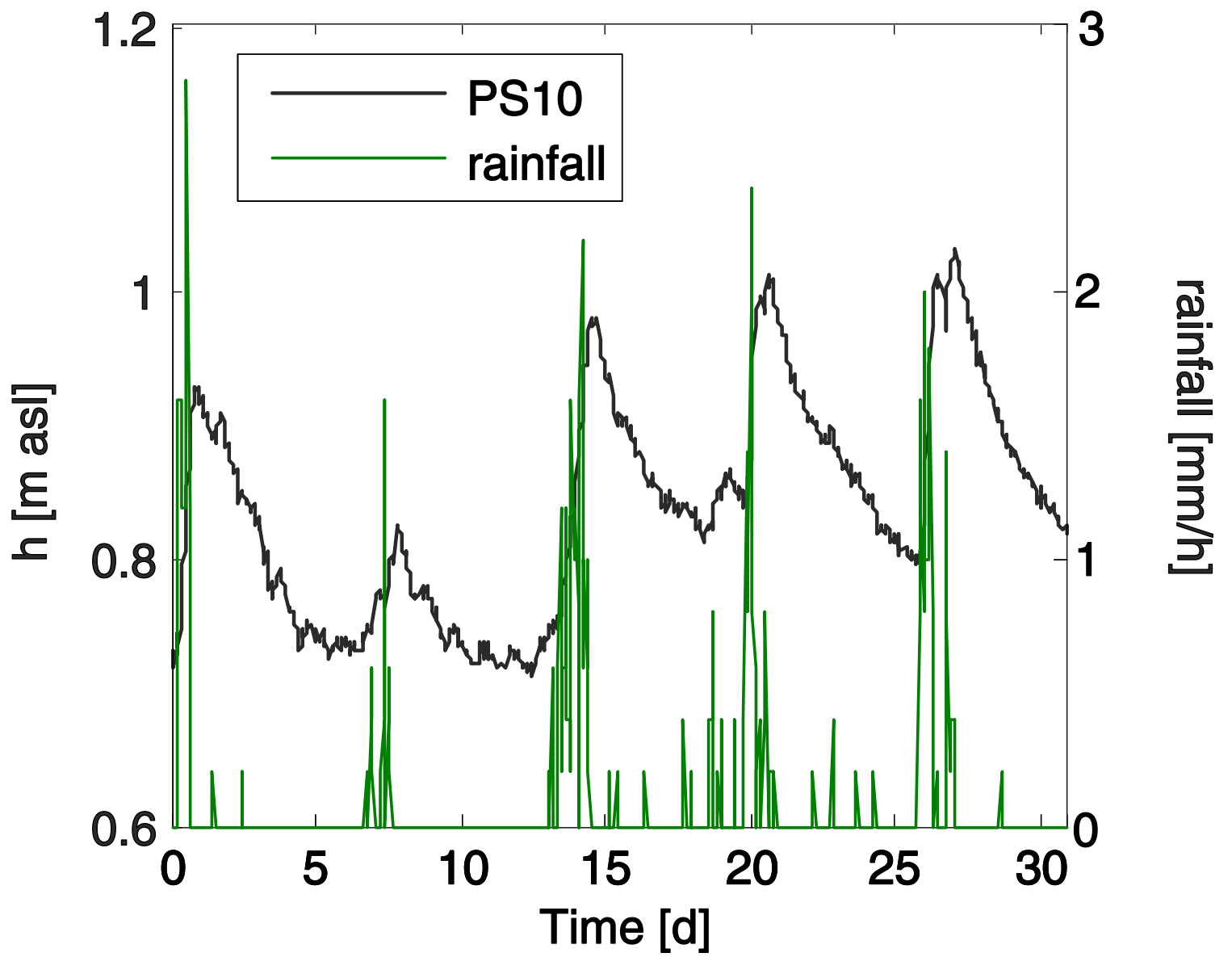


Figure 7
[Click here to download high resolution image](#)

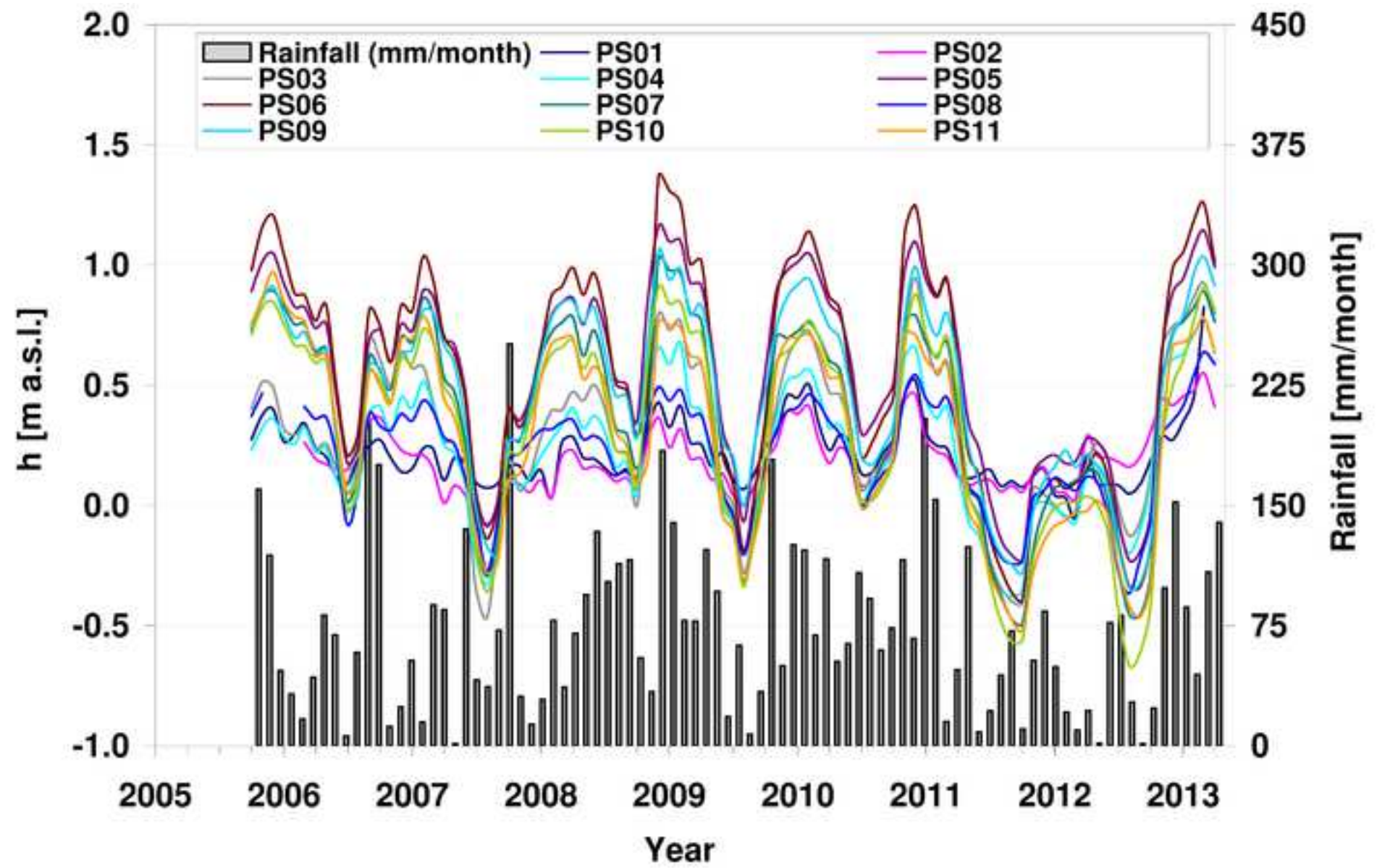


Figure 8

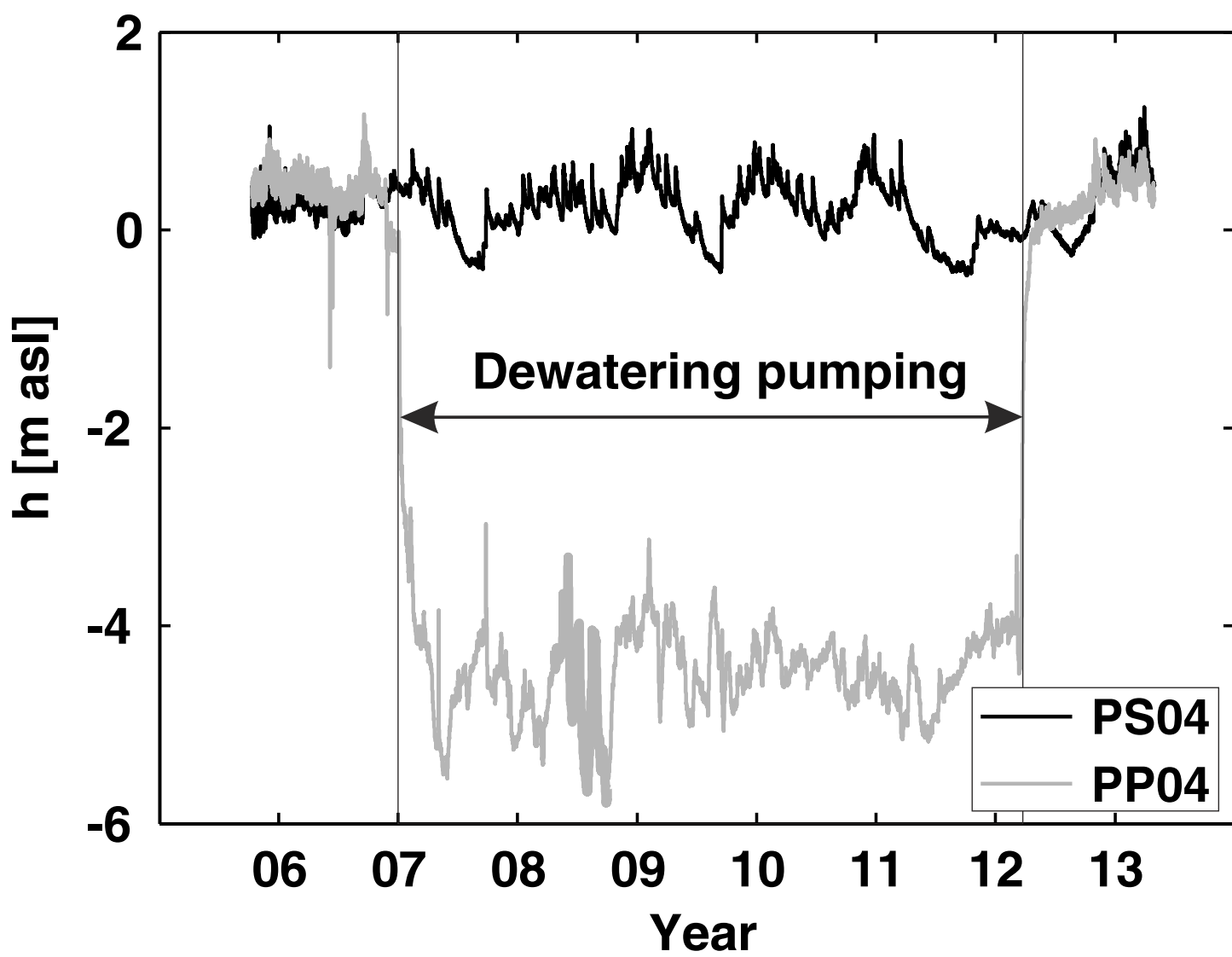


Figure 10

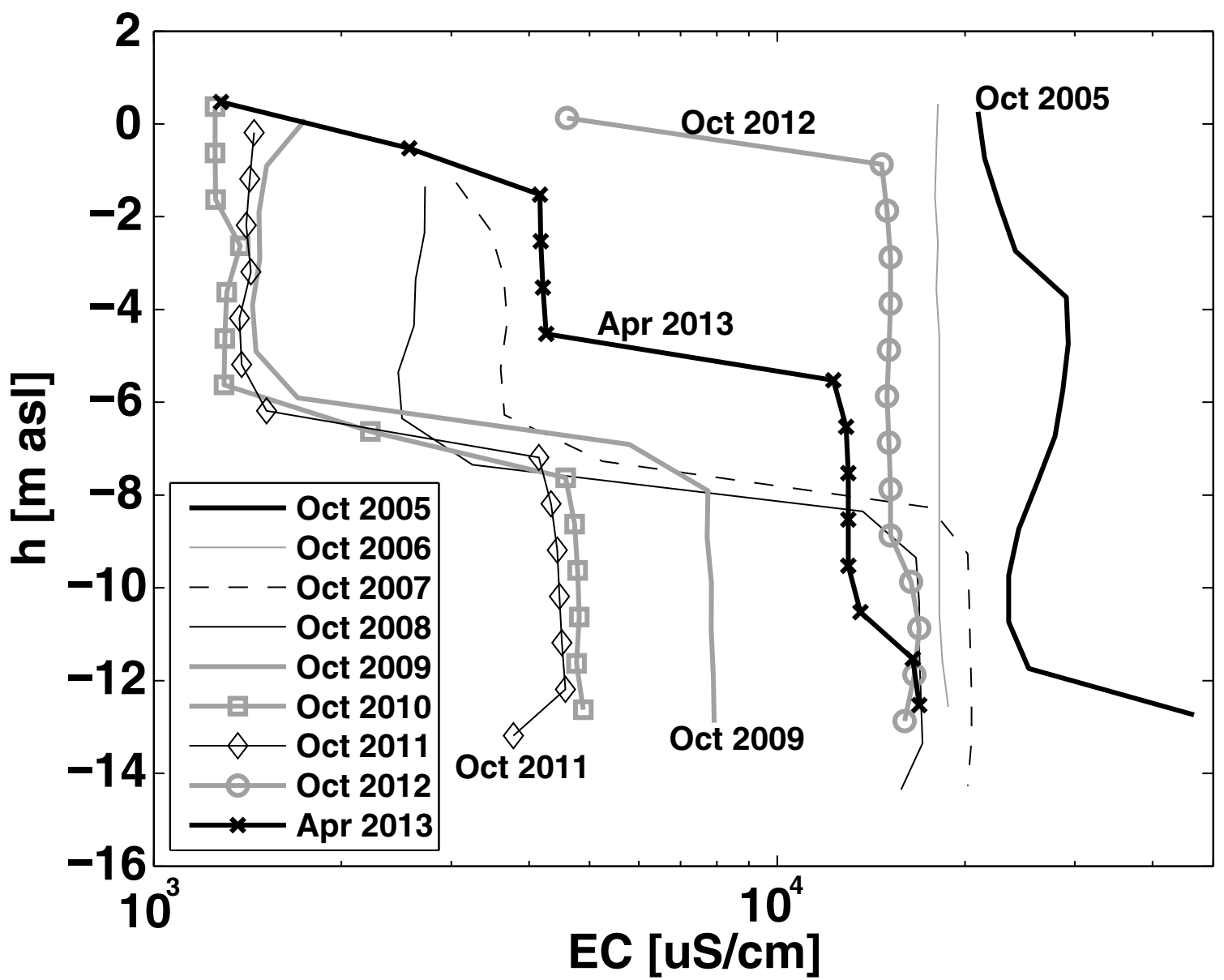
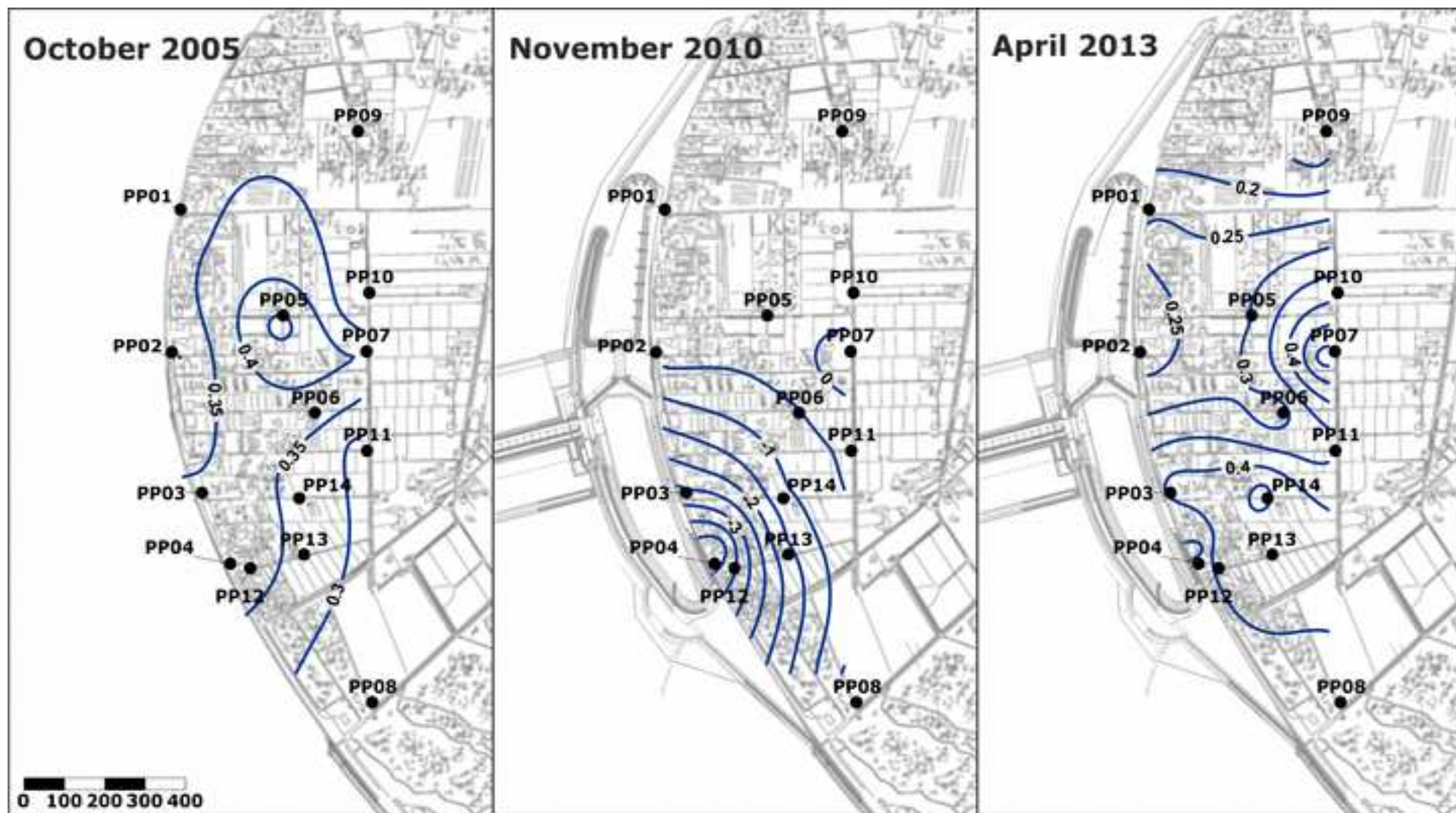


Figure 11
[Click here to download high resolution image](#)



Supporting information

[Click here to download Supplementary Material: 2014_02_25_Supporting information.doc](#)